

Integrated Mach–Zehnder interferometer based on ARROW structures for biosensor applications

F. Prieto^{a,*}, B. Sepúlveda^a, A. Calle^a, A. Llobera^b,
C. Domínguez^b, L.M. Lechuga^a

^aBiosensors Group, Centro Nacional de Microelectrónica, IMM-CNM, CSIC, Isaac Newton 8 (PTM), 28760 Tres Cantos, Madrid, Spain

^bBiosensors Group, Centro Nacional de Microelectrónica, IMB-CNM, CSIC, Campus UAB, 08193 Bellaterra, Barcelona, Spain

Received 12 July 2002; received in revised form 28 December 2002; accepted 10 January 2003

Abstract

The theoretical design, fabrication and characterisation of an evanescent field integrated optical (IO) sensor based on a rib anti-resonant reflecting optical waveguide (ARROW) structure are presented. The optical waveguides are designed to verify two conditions: mono-mode behaviour and high surface sensitivity. The sensor system is fabricated with ‘silicon microelectronics technology’ and it has been tested as a refractometer with glucose solutions of different refractive indices. The feasibility of applying the sensor for immunosensing is shown with antibody/antigen binding experiments.

© 2003 Elsevier Science B.V. All rights reserved.

Keywords: ARROW; Evanescent field sensors; Mach–Zehnder interferometer; Silicon technology

1. Introduction

Integrated optical (IO) devices are increasingly been used as transducers for opto-chemical sensing applications [1,2]. IO devices combine high sensitivity, mechanical stability, miniaturisation and the possibility of mass-production. Use of standard silicon microelectronics technology for the fabrication of these devices allows a high homogeneity of the waveguide material and the possibility of integration of the optical and electrical functions on one single chip.

In order to develop a highly sensitive optical transduction scheme at reasonable cost, we have developed optical evanescent field sensors based on anti-resonant reflecting optical waveguides (ARROW) structures as optimised transducers for biosensing. In the ARROW configuration, light confinement is based on anti-resonant reflections rather than total internal reflection (TIR). These waveguides exhibit low losses and permit larger dimensions than conventional waveguides (micrometers instead of nanometers), an important subject for further technological development and mass-production of the sensors. They have good discrimination against higher order modes and, therefore, show virtual

mono-mode behaviour. Moreover, they show a selective behaviour in polarisation and wavelength and a high tolerance for the selection of the refractive index and thickness of the interference layers.

Among the different techniques that can be employed for the transduction principle, we have chosen interferometry due to its inherent high sensitivity and accuracy. In the Mach–Zehnder interferometer (MZI) integrated version [3], an optical waveguide is split into two arms and after a certain distance they are recombined again (see Fig. 1). One of the branches, the sensor arm, will be exposed to a variation of the optical properties of the outer medium (i.e. refractive index) during a certain distance L (interaction length). During this distance, the guided mode in the sensing arm will experience a phase shift respect to the reference arm guided mode. At the Y-junction output, light coming from both branches will interfere showing a sinusoidal variation related to the change of the refractive index of the surrounding medium. Due to the possibility of fabrication of MZI with interaction lengths of several centimetres, this interferometer configuration presents a high sensitivity.

The sensors based on ARROW structures [4] are fabricated with standard silicon microelectronics technology at our Clean Room facilities using a CMOS compatible process. The guiding layer consists of a ridge structure of non-stoichiometric silicon dioxide (SiO_x) deposited using a

* Corresponding author.

E-mail address: francisco@imm.cnm.csic.es (F. Prieto).

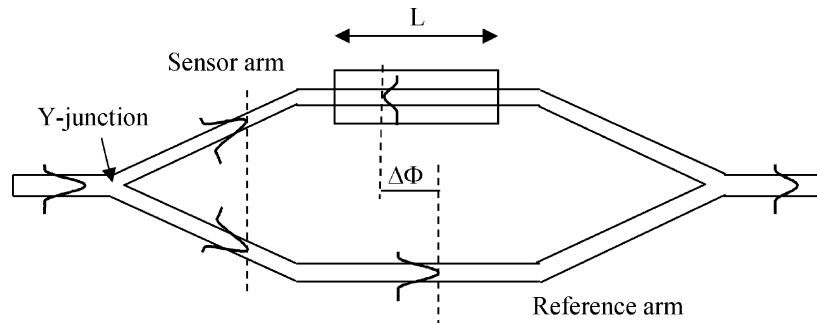


Fig. 1. Scheme of an integrated Mach-Zehnder interferometer.

technology [5] that allows the precise control on the refractive index ranging from 1.46 to 1.90 (depending on x).

We have performed the design, fabrication and characterisation of the channel ARROW Mach-Zehnder Interferometer. For the measurements of the sensor system, we have designed and fabricated macro- and micro-flow cells to introduce the samples into the sensor area. The micro-flow cell, with the same dimensions as the MZI sensor, has been fabricated with silicon micro-machining techniques and is incorporated by fusion bonding to the sensor structure. The complete system will be employed for immunochemical evaluations.

2. The ARROW structure

Conventional TIR waveguides are well known structures that have been used previously for the development of integrated optical sensors [6]. For implementation in an integrated Mach-Zehnder interferometer they should be designed for mono-mode behaviour, that can be controlled with the proper selection of the refractive index, thickness and rib depth of the core layer. Typical dimensions of the core to obtain single-mode behaviour are in the order of hundreds of nanometers (~ 100 nm), with rib depths of only a few nanometers (~ 3 nm) [6]. This is a drawback from a technological point of view because, depending on the deposition process, the rib depth can be of the same size of the surface roughness. Moreover, these small dimensions mean high insertion losses when coupling light directly from a laser source or an optical fibre.

To overcome these problems we propose the use of ARROW structures because it is possible to obtain mono-mode behaviour with core dimensions in the order of micrometers (ARROW) instead of nanometres (TIR), important subject for future mass-batch production of the devices. Also, the greater dimension of the core implies lower insertion losses.

Anti-resonant reflecting optical waveguide is a five-layer guiding structure where light is confined within the core layer by total internal reflection at the outer medium–core interface and by anti-resonant reflection (reflectivity of around 99.96%) at the two interference cladding layers

underneath the core, as it is shown in Fig. 2 [4]. The interference cladding confers special features to the waveguide: ARROW is a leaky structure with virtual mono-mode behaviour, where higher order modes are filtered out by loss discrimination due to the low reflectivity at the interference cladding for these modes. Moreover, TE-polarised light has lower losses than TM-polarised light due to the presence of the high refractive index cladding layer. The refractive indexes and thickness of the cladding layers have to be properly designed for the working wavelength to assure high reflectivity and, therefore, good guiding characteristics. The ARROWS that we have designed and fabricated are based on silicon technology and the materials used are silicon for the substrate, silicon oxide for the core and second cladding layers and silicon nitride for the first cladding. In the original ARROW structure [4], the material used for the core and second cladding is silicon oxide with a refractive index of 1.46. However, we propose a new structure, called modified-ARROW-A, where the core has a refractive index higher than the second cladding. The reason for this asymmetric structure is that, for sensor applications, the Mach-Zehnder interferometer has to be locally protected with a covering layer (with a refractive index of 1.46). To confine light in the core layer, its refractive index has to be higher (i.e. 1.485).

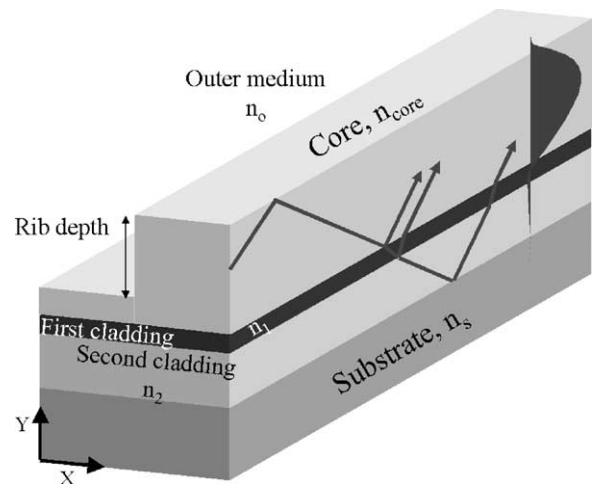


Fig. 2. ARROW structure showing the different waveguide layers and operation principle.

This new structure is less dependent on polarisation and presents lower attenuation losses than the original ARROW structure. A drawback is that it can lose the virtual single-mode behaviour depending on the core dimensions, being possible the propagation of several higher order modes for certain excitation conditions.

3. Sensitivity for ARROW structures

To assure a high sensor response for changes in the optical properties of the outer medium, the optical waveguide has to be designed with a high surface sensitivity. Surface sensitivity, calculated for processes that involve the adsorption of molecules from a gaseous or liquid phase, is defined as the rate of change of the effective refractive index of the guided mode, N , as the thickness of the homogeneous molecular adlayer, d_1 , varies [7,8]. This sensitivity is related to the squared field magnitude of the guide mode at the core–outer medium interface, considering a homogeneous adsorbed layer of refractive index n_1 and thickness d_1 . We have developed the analytical expression of surface sensitivity for an ARROW structure, which takes the form [9]:

$$\frac{\partial N}{\partial d_1} \approx \frac{\gamma_o}{N} \left[\left(\frac{n_1}{n_o} \right)^{2\rho} \gamma_o^2 - \left(\frac{n_o}{n_1} \right)^{2\rho} \gamma_1^2 \right] \frac{P_0}{P_T} \quad (1)$$

with $\rho = 0$ for TE modes and $\rho = 1$ for TM modes, where $\gamma_i = k_0 \sqrt{N^2 - n_i^2}$ ($i = o, 1$), n_1 is the refractive index of the

adsorbed adlayer, n_o the refractive index of the outer medium, P_0 the power of the guided mode at the cover medium and P_T the total power of the guided mode [9]. Using a home-made computational program based on the non-uniform finite difference method (UN-FDM) [10], surface sensitivity has been evaluated as a function of the thickness and refractive index of the core and results are presented in Fig. 3 for the TE and TM polarisation. The maximum obtained values are in the order of $0.06 \times 10^{-4} \text{ nm}^{-1}$ for TE polarisation, almost two orders of magnitude respect to the highest values presented for TIR waveguides ($3.4 \times 10^{-4} \text{ nm}^{-1}$) [6].

This is the main disadvantage that ARROW structures present respect to TIR waveguides: due to the intrinsic characteristics of ARROW, the guided mode is quite confined within the core layer, and, therefore sensitivity is very low. To increase surface sensitivity for ARROW structures we have proposed several alternatives [9]. (a) Decrease the refractive index of the core layer, although we are limited by the refractive index of the protective layer, i.e. 1.46. (b) Sensitivity is also increased if the thickness of the core diminishes; however, the advantage of ARROW versus TIR is lost if the core thickness decreases from micrometer dimensions. (c) The best alternative to increase sensitivity of ARROW structures more than one order of magnitude is to incorporate a high refractive index thin film over of the core layer [11]. As it is shown in Fig. 4, for overlay thickness of several tens of nanometer, sensitivity shows an important increment due to the distortion that the overlay introduces in the fundamental guided mode, increasing the field penetra-

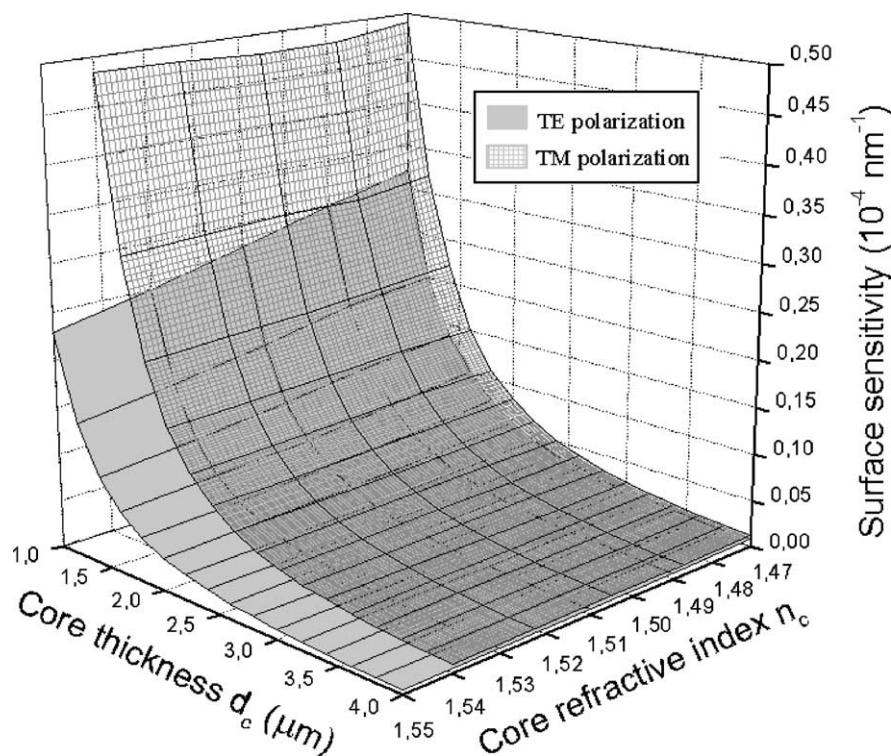


Fig. 3. Surface sensitivity for the adsorption of molecules ($n_1 = 1.45$) from an aqueous solution ($n_o = 1.33$) on the waveguide surface vs. core thickness. The ARROW structure has a core refractive index of 1.485.

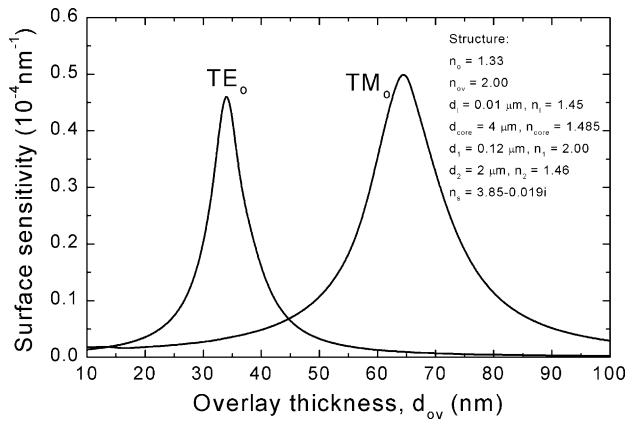


Fig. 4. Sensitivity vs. overlay thickness for the TE_0 and TM_0 modes of an ARROW structure with a core thickness of $d_{\text{core}} = 4 \mu\text{m}$ and refractive index of $n_{\text{core}} = 1.485$.

tion into the cover medium. Using the high refractive index overlay, sensitivity for ARROW structures is only a factor 4 lower than for TIR waveguides.

4. Sensor configuration

The optical waveguides that will form the Mach–Zehnder interferometer sensor must verify two important conditions: mono-mode behaviour and high surface sensitivity. To theoretically evaluate these characteristics, we have used the home-made one-dimensional computational program based on the non-uniform finite difference method [10].

Attenuation losses for several modified-ARROW-A configurations, with different core refractive indexes and core thickness, have been evaluated. For a given core thickness, as the core refractive index increases, attenuation losses decreases for the fundamental TE_0 and TM_0 modes [11]. However, higher order modes also present lower losses being possible that the ARROW would support several modes. We must choose a combination of core refractive index and thickness in order to obtain single-mode behaviour in the vertical direction (y-axis in Fig. 2). To confine light in the lateral direction (x-axis in Fig. 2) a rib structure is designed. Attenuation losses as well as single-mode behaviour will depend on the width and depth of the rib. We observed good lateral confinement for rib depths in the order of 60% of the core thickness [12]. Regarding the rib width, a lateral dimension lower than $8 \mu\text{m}$ would be enough to obtain lateral mono-mode behaviour.

Summarising the previous results, for the design of ARROW structures for sensor applications, we must come to an agreement between single-mode behaviour, low attenuation losses for the fundamental mode and high surface sensitivity. For those reasons, the multi-ARROW-A configuration that has been finally chosen, for an operating wavelength of $0.633 \mu\text{m}$, has the following structure: silicon substrate; $2 \mu\text{m}$ thick silicon dioxide second cladding ($n_2 = 1.46$); $0.12 \mu\text{m}$ silicon nitride first cladding ($n_1 = 2.00$); and a silicon oxide

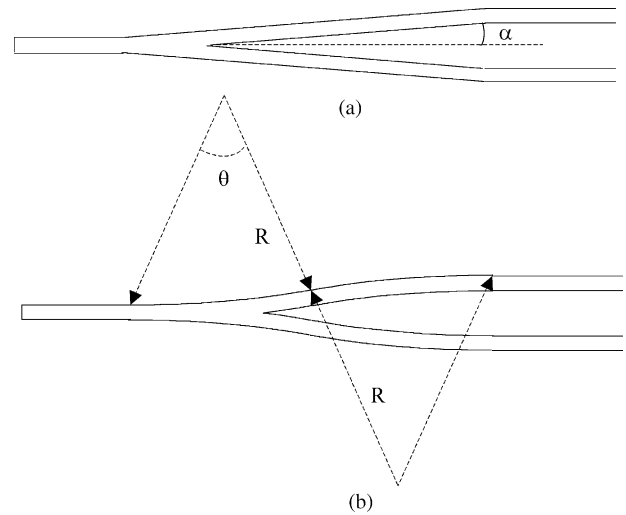


Fig. 5. Different types of designed and fabricated Y-junctions: (a) straight arms; (b) circular arms.

core layer with a refractive index of 1.485 and thickness varying from 1.5 to $4 \mu\text{m}$. The rib depth was set to the 60% of the core thickness and the rib width was chosen below $8 \mu\text{m}$ ($4\text{--}7 \mu\text{m}$) to assure mono-mode behaviour.

To study the sensitivity of the waveguides, a silicon nitride layer ($n_{\text{ov}} = 2.00$) with thickness of 40, 60 and 120 nm was deposited over the core layer. Finally, the devices are covered with a silicon oxide protective layer ($n_p = 1.46$) with thickness of $2 \mu\text{m}$.

As it was mentioned before, the design of the sensor structure, it is based on the Mach–Zehnder configuration. In the integrated version of the MZI, an optical waveguide is split into two arms and after a certain distance they recombine again [3]. The interferometer is covered with a protective layer and an area of length L is opened in one of the arms (sensor arm) to bring into contact the waveguide and the environment. Only light travelling in the sensor arm will experience a phase shift induced by a change in the properties of the surrounding medium.

Several MZI configurations were designed varying the separation between arms and the Y-junction parameters. All the devices are symmetric with two different divisor shapes: in the first case the Y-junction is formed with straight arms and opening angle of 1° (see Fig. 5a). In the second case, the divisor is shaped with circular bends with radii of 5, 20 and 80 mm (see Fig. 5b). In all cases, the separation between the sensor and reference arms is of $100 \mu\text{m}$ to avoid coupling between modes travelling through both branches. In one arm, a sensor area with different lengths (6, 10, 15 and 20 mm) is created. The total length of the device is 35 mm .

5. Fabrication of the sensor

The devices are fabricated in our Clean Room facilities using a silicon CMOS compatible process [13]. The process

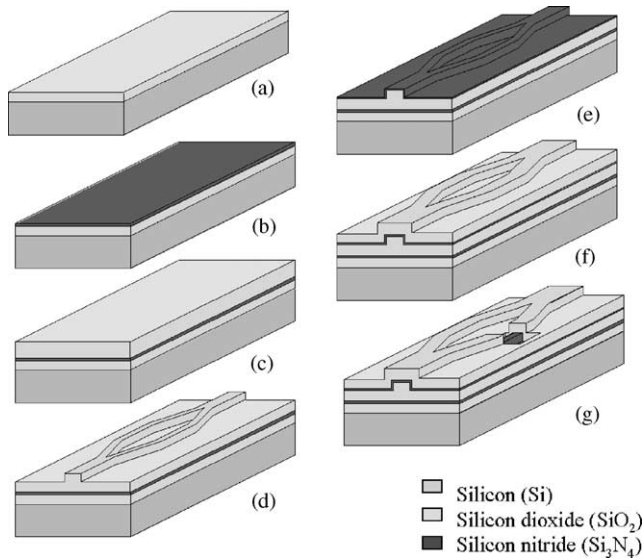


Fig. 6. Fabrication process at the Clean Room of the integrated MZI sensor.

is described in Fig. 6. The waveguide substrate is silicon ($n_s = 3.85 - j0.019$ at the working wavelength of 632.8 nm). The second cladding is a Thermally grown silicon dioxide (SiO_2) layer with a refractive index of 1.46 and a thickness of 2 μm (Fig. 6a). The first cladding is a silicon nitride (Si_3N_4) layer with a thickness of 0.12 μm and a refractive index of 2.00 deposited by low pressure chemical vapour deposition (LPCVD) at 800 $^\circ\text{C}$ (Fig. 6b). Finally, the waveguide core is a

non-stoichiometric silicon oxide (SiO_x) layer with a refractive index that can be modulated according to x (Fig. 6c). The technology of growing SiO_x by plasma enhanced chemical vapour deposition (PECVD) has been developed previously in our group [5] and we are capable of varying the refractive index between 1.46 and 1.9, depending on x . The core thickness is varied between 1.5 and 4 μm . To obtain lateral confinement of light, a rib structure is defined. The rib depth is designed to be around 60% of the core thickness to obtain good confinement of light. The rib is defined on the core layer by reactive ion etching (RIE) (Fig. 6d). Several devices were designed with different widths, ranging from 4 to 7 μm , to experimentally analyse its influence in the guiding properties of the structure.

The overlay is a silicon nitride (Si_3N_4) layer with a thickness of 40, 60 or 120 nm deposited by LPCVD at 800 $^\circ\text{C}$, analogous to the first cladding layer (Fig. 6e). The protective layer is a non-stoichiometric silicon oxide layer with a refractive index of 1.46 deposited by PECVD at 300 $^\circ\text{C}$ (Fig. 6f). The thickness of this layer is 2 μm , enough to isolate the core from the environment. A sensing window of length L is opened in one of the interferometer branches. The opening of the sensor area in the protective layer is done, after a photolithographic process, by chemical etching with a $\text{HF}:\text{H}_4\text{NF}$ (1:7) solution (Fig. 6g). Finally, the sensors are cut in individual pieces and polished for light coupling by end-face. The total length of the sensor is 35 mm. Fig. 7 shows a picture of one of the fabricated chips with 14 different sensors.

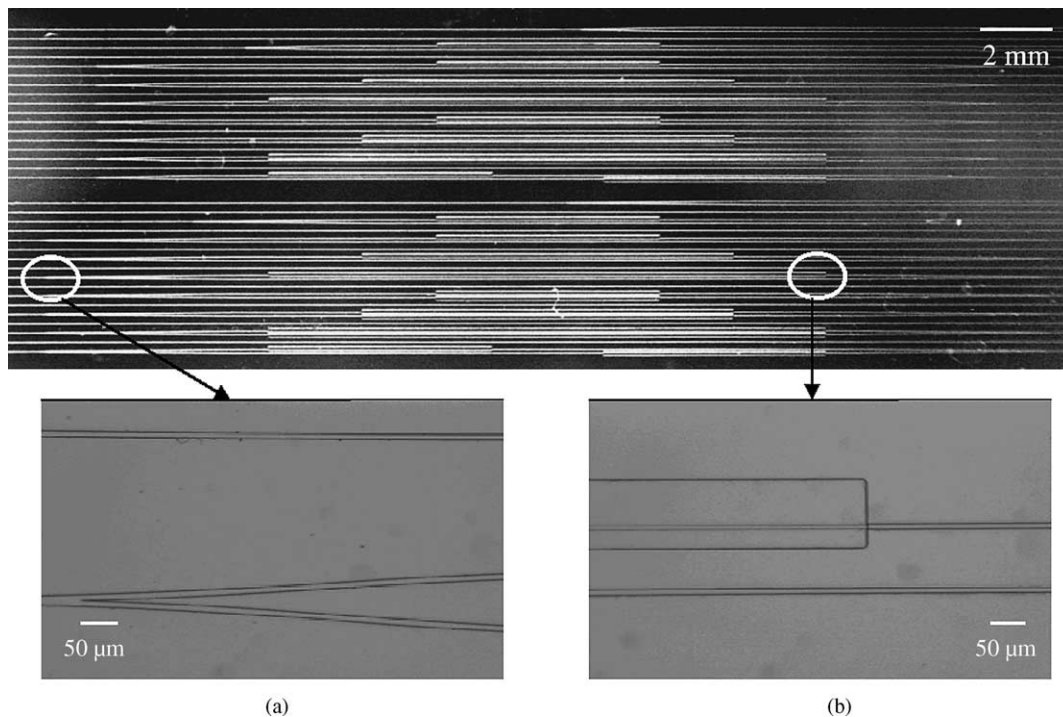


Fig. 7. Picture of one of the fabricated chips containing the different designed devices (sensors, Y-junctions and straight waveguides): (a) Y-junction; (b) sensor area.

6. Optical characterisation

The optical characterisation is performed with TE-polarised light from a He:Ne laser ($\lambda = 0.633 \mu\text{m}$) that is coupled to a single-mode optical fibre (3.8 μm core diameter) using a microscope objective (40 \times) [11]. The optical fibre has a small length (around 15 cm) and is placed in straight line to preserve the input TE-polarisation. The end of the mono-mode fibre is placed in front of the waveguide rib face to couple light into the ARROW structure (end-fire coupling). Light is collected by a multi-mode standard optical fibre (50 μm core diameter) connected to a silicon photodiode. Precise translation stages are used for the accurate alignment of all the components. A synchronous detection scheme is used with the aid of a lock-in amplifier and a light chopper. Finally, home-made software is available for collecting the measurement data. Alternatively, a microscope objective (100 \times) and a silicon CCD camera are used to study the field distribution at the end of the waveguide.

The sensor is being developed for the detection of biochemical interactions between a receptor molecule and its complementary analyte. The effect of this reaction is comparable to a change of the bulk refractive index of the outer medium. Therefore, the use of solutions with different refractive indexes is useful for studying the sensor sensitivity. Several solutions were prepared with different glucose concentrations in water, with refractive indexes varying from 1.3325 to 1.4004 (± 0.0002), as determined by an Abbe refractometer operating at 25 $^{\circ}\text{C}$. A flow cell mechanised in Teflon (with a channel width of 3 mm, a depth of 100 μm and a length of 15 mm) is clamped onto the interferometer and a flow injection system is used to deliver the glucose solutions into the sensor area.

Using as a reference the refractive index of deionised (DI) water ($n = 1.3325$), different glucose solutions with varying

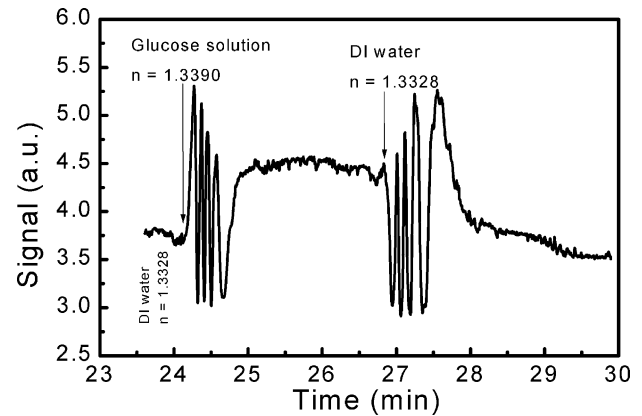


Fig. 8. Sensor response for a change of the refractive index in the sensor area. The sensor has been tested with glucose solutions of different refractive indices.

refractive indexes were introduced alternatively, as it is shown in Fig. 8. With these measurements, a calibrating curve was evaluated where the phase response of the sensor is plotted versus the variation in the refractive index. Fig. 9 shows these calibrating curves for four different MZI sensors using TE polarisation. For a sensor with a core thickness of 4 μm , sensor area of length $L = 6 \text{ mm}$ and the overlay thickness of 120 nm (solid circle in Fig. 9) sensitivity is very low, as theory predicts [9] due to the high confinement of the mode within the core.

However, if the overlay thickness is decreased to some tens of nanometers, sensitivity is enhanced more than an order of magnitude [11]. The sensors fabricated with overlay thickness lower than 120 nm have excessive propagation losses and they were discarded. Therefore, to increase sensitivity we decided to etch locally the silicon nitride protective layer at the sensor area to a value close to 34 nm, where the theory predicts that sensitivity is maximum (see Fig. 4). The etching was performed in a H_3PO_4 bath at

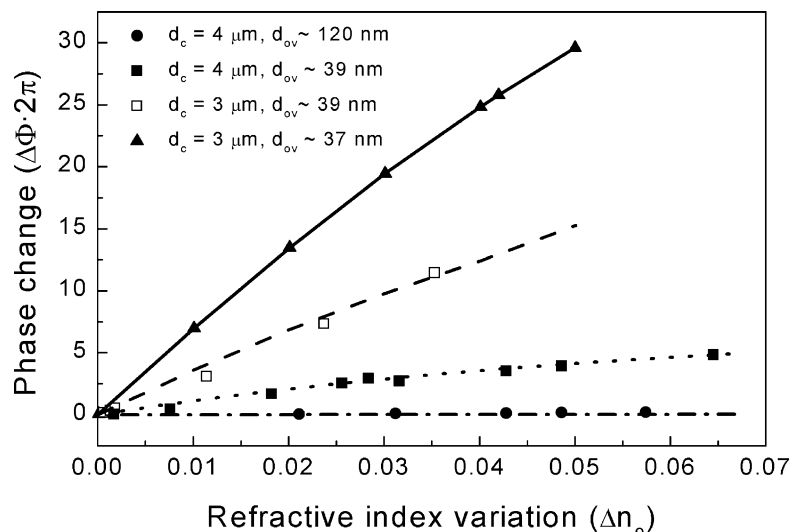


Fig. 9. Calibrating curves for the MZI-ARROW sensor with different waveguide structures (see inset) (TE polarisation).

180 °C (etch rate 10 nm min⁻¹). After the etching process, the thickness of the silicon nitride layer was diminished to, approximately, 39 nm (measured with a profilograph). Measurements with the MZI sensor (core thickness of 4 µm and sensor area of length $L = 6$ mm) are shown in Fig. 9 (solid square), where we can observe the sensitivity enhancement due to the high refractive index thin layer.

Sensitivity can also be increased if the core thickness diminishes because the guided mode is less confined within the core [9]. For a sensor with 3 µm of core thickness, interaction length $L = 10$ mm and an overlay thickness of 39 nm (open square in Fig. 9), the refractive index detection limit is one order of magnitude higher than before ($\Delta n_{o,min} = 1 \times 10^{-4}$ or $\Delta N = 2 \times 10^{-6}$).

Finally, as it is shown in Fig. 4, for small variations of the overlay thickness, sensitivity can be increased significantly. A variation of only 2 nm in this overlay (37 nm, solid triangle in Fig. 9) implies a sensitivity increment of almost one order of magnitude. In this case, for a MZI sensor with 3 µm of core thickness and a sensor area length of 15 mm, the maximum sensitivity obtained is $d\Delta\Phi(2\pi)/dn = 480$, which corresponds to a minimum detectable refractive index variation of $\Delta n_{o,min} = 2 \times 10^{-5}$ ($\Delta N = 4 \times 10^{-7}$).

In these measurements, we used a macro-flow cell mechanised on Teflon (with a channel width of 3 mm and a channel depth of 100 µm). In order to achieve a more compact device and to increase the diffusion rate of the analytes, a new silicon micro-flow cell has been fabricated. This micro-flow cell has the same dimensions as the sensor area (6 mm long and 100 µm wide) with a channel depth of 50 µm ($V = 30$ µl) and has been fabricated by silicon micro-machining techniques: etching of silicon with a 20% KOH stirring solution at 80 °C to obtain the channel and holes. This micro-flow cell will be fixed on top of the sensor by fusion bonding and will be used in further measurements.

7. Biosensing applications

As an example of biosensing application we have used the sensor for the detection of the immunoreaction antibody/antigen α -HSA/HSA (human serum albumin, antibody A0433, antigen A9511 Sigma). The measurements have been performed with a MZI-ARROW sensor with 3 µm of core thickness, an interaction length of 15 mm and an overlay thickness of 37 nm.

In Fig. 10, we present the results of the detection of the immunoreaction α -HSA/HSA. Fig. 10a shows the physical adsorption of the antibody α -HSA on the sensor surface. We introduced an Ab concentration of 0.015 mg ml⁻¹ in a buffer solution (phosphate buffered saline, PBS) of pH 7.35 at a constant flow rate of 20 µl min⁻¹. We can observe that the phase change in the first part of the process is fast and, as the surface is more occupied, the phase response $\Delta\Phi$ varies more slowly. After complete adsorption, the total phase change is $4.4 \times 2\pi$, that corresponds to the adsorption of

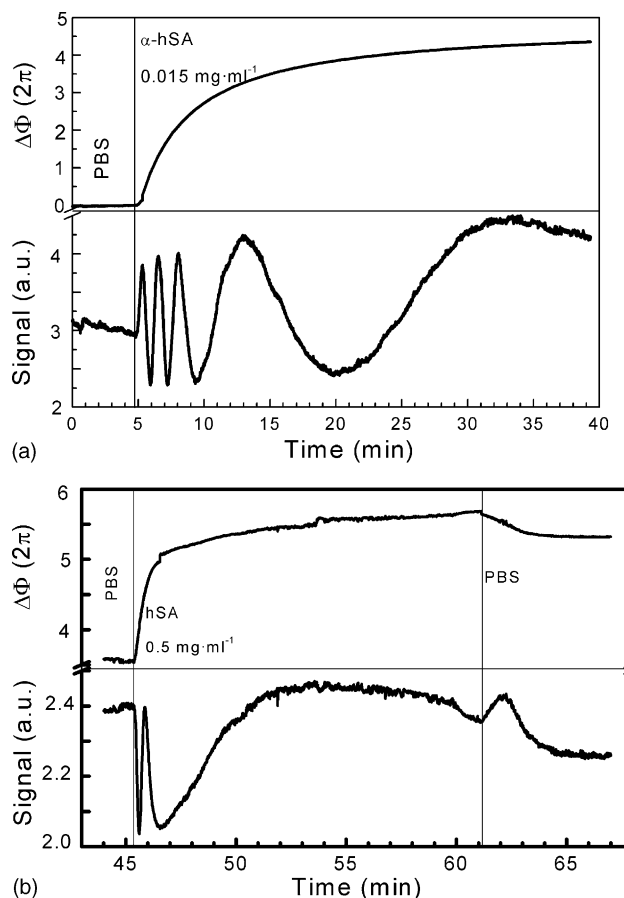


Fig. 10. Signal response (TE polarisation) of the MZI-ARROW sensor to the antigen/antibody α -HSA/HSA immunoreaction. (a) Physical adsorption of the α -HSA antibody; (b) immunoreaction with the antigen HSA.

a homogeneous Ab monolayer of average thickness $d_1 \approx 4$ nm (surface covering of 2.4 ng mm⁻² [14]).

After rinsing with PBS, the non-adsorbed antibodies are washed out, being the net sensor response equivalent to an average thickness of $d_1 \approx 3$ nm, that corresponds to a surface coverage of 1.8 ng mm⁻². Subsequently, we add a bovine serum albumin (BSA) concentration of 0.5 mg ml⁻¹ to block the empty sites in the sensor surface. This process implies a growth in the average thickness of the adsorbed protein monolayer to $d_1 \approx 4$ nm. Finally, a concentration of 7.7×10^{-6} M human serum albumin antigen (HSA) is flowed through the sensor, giving an additional increment of the protein monolayer of $d_1 \approx 1.8$ nm (Fig. 10b) due to the immunoreaction.

These experiments show the feasibility of using the MZI sensor for the direct detection of selective molecular interactions.

8. Conclusions

For the development of a highly sensitive integrated optical sensor based on the Mach-Zehnder interferometer

configuration it is necessary to design optical waveguides that verify two conditions: mono-mode behaviour and high surface sensitivity. ARROW structures based on silicon technology meet these requirements under certain conditions.

In this paper, we have first evaluated, theoretically, the different conditions necessary to obtain single-mode ARROW structures. Second, we present the results with the MZI sensors based on the designed structures. To obtain devices with higher sensitivity, a high refractive index thin overlay is deposited on top of the ARROW core. We have performed a theoretical analysis of the optimal overlay thickness that gives the greatest sensitivity enhancement and new devices have been designed and tested.

This optimised waveguide consist on a rib-ARROW structure with a silicon oxide core layer ($n_{\text{core}} = 1.485$) and thickness higher than $2\text{ }\mu\text{m}$; a silicon oxide second cladding layer with a refractive index of 1.46 and a fixed thickness of $2\text{ }\mu\text{m}$ and a silicon nitride first cladding layer, $0.12\text{ }\mu\text{m}$ thick, with a refractive index of 2.00. The waveguide is overcoated with a thin silicon nitride layer ($n_{\text{ov}} = 2.00$) and with a silicon oxide layer ($n = 1.46$) with a thickness of $2\text{ }\mu\text{m}$. The rib depth is 60% of the core thickness and the rib width should be lower than $8\text{ }\mu\text{m}$ to obtain single-mode behaviour.

Several MZI configurations were fabricated to analyse experimentally the more appropriate sensor design. To increase the surface sensitivity, we have propose the local etch of the silicon nitride overlay to values close to 34 nm . These sensors have been characterised as refractometers, obtaining a refractive index detection limit of $\Delta n_{\text{o,min}} = 2 \times 10^{-5}$. This limit is around a factor 4 lower than the limit obtained with a TIR-MZI fabricated with the same technology [6]. Finally, we have demonstrated that it is feasible to use the sensor for the direct detection of the immunoreaction antibody/antigen α -HSA/HSA.

Acknowledgements

This work was supported by the Comisión Interministerial de Ciencia y Tecnología (projects TIC97-0594-C04-01 and

AMB98-1048-C04-02) and by the Comunidad Autónoma de Madrid (project CAM-07M/0051/1999).

References

- [1] R.P.H. Kooyman, L.M. Lechuga, in: E. Kress-Rogers (Ed.), *Handbook of Biosensors and Electronic Noses*, CRC Press, New York, 1997, Chapter 8, pp. 169–196.
- [2] P.V. Lambeck, Integrated opto-chemical sensors, *Sens. Actuators B* 8 (1992) 103–116.
- [3] R. Syms, J. Cozens, *Optical Guided Waves and Devices*, McGraw-Hill, London, 1992.
- [4] M.A. Duguay, Y. Kokubun, T.L. Koch, Antiresonant reflecting optical waveguides in SiO_2 -Si multilayer structures, *Appl. Phys. Lett.* 49 (1986) 13–15.
- [5] C. Domínguez, J.A. Rodríguez, F.J. Muñoz, N. Zine, Plasma enhanced CVD silicon oxide films for integrated optic applications, *Vacuum* 52 (1999) 395–400.
- [6] E.F. Shipper, A.M. Brugman, C. Domínguez, L.M. Lechuga, R.P.H. Kooyman, J. Greve, The realization of an integrated Mach-Zehnder waveguide immunosensor in silicon technology, *Sens. Actuators B* 40 (1997) 147–153.
- [7] K. Tiefenthaler, W. Lukosz, Sensitivity of grating couplers as integrated-optical chemical sensors, *J. Opt. Soc. Am. B* 6 (1989) 209–220.
- [8] O. Parriaux, G.J. Veldhuis, Normalized analysis for the sensitivity optimization of integrated optical evanescent-wave sensors, *J. Lightwave Technol.* 16 (1998) 573–582.
- [9] F. Prieto, A. Llobera, D. Jiménez, C. Domínguez, A. Calle, L.M. Lechuga, Analysis of silicon antiresonant reflecting optical waveguides for evanescent field sensors, *J. Lightwave Technol.* 18 (2000) 966–972.
- [10] C.M. Kim, R.V. Ramaswamy, Modeling of graded-index channel waveguides using nonuniform finite difference method, *J. Lightwave Technol.* 7 (1989) 1581–1589.
- [11] F. Prieto, L.M. Lechuga, A. Calle, A. Llobera, C. Domínguez, Optimised silicon antiresonant reflecting optical waveguides for sensing applications, *J. Lightwave Technol.* 19 (2001) 75–83.
- [12] I. Garcés, F. Villuendas, J.A. Vallés, C. Domínguez, M. Moreno, Analysis of leakage properties and guiding conditions of rib antiresonant reflecting optical waveguides, *J. Lightwave Technol.* 14 (1996) 798–805.
- [13] M. Moreno, I. Garcés, J. Muñoz, C. Domínguez, J. Calderer, F. Villuendas, J. Pelayo, CMOS compatible ARROW guides, in: *Proceedings of the 8th CIMTEC*, S-VII.2, Florence, Italy, 1994.
- [14] J.A. De Feyter, J. Benjamins, F.A. de Veer, Ellipsometry as a tool to study the adsorption behaviour of synthetic and biopolymers at the air–water interface, *Biopolymers* 17 (1978) 1759–1772.